endothelial cell proliferation via suppressing VEGF receptor 1 (Flt-1) and 2 (Flk/KDR) expression in vitro.[5] Likewise, there are controversial reports regarding in vivo neovascularization using different TZDs in different models.[6–8] Pioglitazone exerts therapeutic angiogenesis in vivo in hindlimb ischemia in a murine model;[9] however, it remains unclear whether pioglitazone-induced angiogenesis depends solely on PPAR-γ activation in endothelial cells or whether it depends on the improvement of hyperglycemia.

Despite its potential therapeutic effect on ischemic neovascularization, the systemic administration of pioglitazone is hampered by its undesirable side effects, including edema and heart failure, which may be optimized by a novel drug delivery system. Recently, we reported that polylactic–glycolic acid (PLGA) nanoparticles (NP) accumulate in the capillary and arteriolar endothelium after intramuscular injection in murine[10] and rabbit[11] models of hindlimb ischemia. The application of PLGA NP as a drug delivery system for pioglitazone may enhance its therapeutic efficacy and may reduce the possible side effects. In this study, we tested our hypothesis that pioglitazone induces therapeutic neovascularization in a nondiabetic murine model of hindlimb ischemia and that the NP-mediated delivery of pioglitazone enhances the therapeutic efficacy of pioglitazone.

Materials and Methods

Preparation of PLGA NP

We prepared PLGA NP incorporating pioglitazone (Pio-NP; Takeda Pharmaceutical Company Limited, Osaka, Japan) or fluorescein isothiocyanate (FITC) (FITC-NP) via the emulsion solvent diffusion method.[12] PLGA was quickly dissolved in a mixture of acetone and methanol, and pioglitazone or FITC was then added. The resultant polymer-FITC or polymer-pioglitazone solution was emulsified in polyvinyl alcohol solution under stirring at 400 rpm using a propeller-type agitator with 3 blades (Heidon 600G; Shinto Scientific, Japan). After agitating the system for 2 hours under reduced pressure at 40°C, the entire suspension was centrifuged (20 000g for 20 minutes at −20°C). After removing the supernatant, purified water was mixed with the sediment. The wet mixture was then centrifuged again to remove the excess polyvinyl alcohol and the unencapsulated reagent that could not be adsorbed by the surfaces of NP. After repeating this process, the resultant dispersion was freeze-dried under the same conditions. The FITC-NP was 4.2% (wt/vol) FITC and Pio-NP was 3.7% (wt/vol) pioglitazone.

Animal Preparation and Experimental Protocol

The study protocol was reviewed and approved by the Committee on Ethics on Animal Experiments, Kyushu University Faculty of Medicine, and the experiments were conducted according to the Guidelines of the American Physiological Society. All mice were maintained in the Laboratory of Animal Experiments at Kyushu University. After anesthesia with an intraperitoneal injection of ketamine hydrochloride (70 mg/kg) and xyladine hydrochloride (3 mg/kg), we induced unilateral hindlimb ischemia in the mice by ligation and excision of the femoral arteries and veins, as previously described.[10] Immediately after inducing ischemia, the animals were divided into treatment groups and were euthanized on day 21. Hindlimb blood flow measurements were performed using a laser Doppler perfusion imaging (LDPI) analyzer (Moor Instruments, United Kingdom). The LDPI index was expressed as the ratio of the LDPI signal in the ischemic limb compared with that in the normal limb. In protocols 1, 2, and 3, the animals received an intramuscular injection of therapeutic agents into the left femoral and thigh muscles using a 27-gauge needle immediately after inducing ischemia, as indicated (Methods and Figure I in the online-only Data Supplement). In protocol 4, the animals received a daily oral treatment

of pioglitazone or vehicle (Methods and Figure I in the online-only Data Supplement).

Distribution of FITC-NP in Ischemic Hindlimb Tissues

Three, 7, 14, and 21 days after hindlimb ischemia and intramuscular injection of FITC-NP, the gastrocnemius muscle was isolated from ischemic and nonischemic limbs, and the FITC signals were examined under a fluorescent microscope. Frozen cross sections of the muscles 3 days after hindlimb ischemia and intramuscular injection of FITC or FITC-NP were then prepared and examined under a fluorescent microscope (Biozero; Keyence, Co, Osaka, Japan). The nuclei were counterstained with 4′,6-diamidino-2-phenylindole (DAPI; Vector Shield, Vector Labs Ltd, United Kingdom) in some sections. Other sections were stained with anti-mouse platelet/endothelial cell adhesion molecule-1 antibody (CD31; Santa Cruz Biotechnology, Inc, Santa Cruz, CA) as the primary antibody and anti-goat IgG (Alexa 555; Life Technologies, Grand Island, NY) as the secondary antibody.

Histological and Immunohistochemical Analyses

A histological and immunohistochemical evaluation was performed in 5-μm paraffin-embedded sections of the gastrocnemius muscle after hindlimb ischemia. To determine the capillary and arteriolar density, cross sections were stained with anti-mouse platelet endothelial cell adhesion molecule with anti–platelet/endothelial cell adhesion molecule-1 (CD31) antibody as a primary antibody (Santa Cruz Biotechnology, Inc) and anti-goat IgG antibody (Alexa 555; Life Technologies) as a secondary antibody. The nuclei were counterstained with DAPI (Vector Laboratories, Inc, Burlingame, CA) and α-smooth muscle actin antibody (DAKO, Glostrup, Denmark).

### Measurements of Pioglitazone Concentration in the Serum and Muscle Tissue

The pioglitazone concentrations in the serum and the muscle were measured at predetermined time points using liquid chromatography coupled to tandem mass spectrometry. Additional details are provided in the Methods in the online-only Data Supplement.

PPAR-γ Activity Measurement in the Muscle Tissue

Nuclear extracts were prepared from the gastrocnemial muscle homogenates using a nuclear extract kit (NE-PER Nuclear and Cytoplasmic Extraction Reagents; Thermo Fisher Scientific Inc, Rockford, IL) according to the manufacturer's instructions. The protein was measured using a BCA Protein Assay kit (Thermo Fisher Scientific Inc). PPAR-γ activation was assayed using ELISA-based PPAR-γ activation TransAM kit (Active Motif, Rixensart, Belgium), which was used according to the manufacturer's instructions. Ten micrograms of nuclear protein samples were incubated for 1 hour in a 96-well plate coated with an oligonucleotide that contains a PPAR response element domain (5′-AACTAGGTCAAAGGTCA-3′), to which the activated PPAR-γ contained in nuclear extracts specifically binds. After washing, PPAR-γ antibody (1:1000 dilutions) was added to these wells and incubated for 1 hour. After incubation for 1 hour with a secondary horseradish peroxidase–conjugated antibody (1:1000 dilution), specific binding was detected by colorimetric estimation at 450 nm with a reference wavelength of 655 nm.

Polymerase Chain Reaction Array

The total RNA was isolated from the gastrocnemial muscles using an RNeasy Fibrous Tissue Mini kit (QIAGEN Inc, Valencia, CA). cDNA synthesis was performed using 1 μg of the total RNA with a PrimeScript RT reagent kit (Takara-Bio, Inc, Shiga, Japan). For angiogenic factor expression analysis, quantitative real-time polymerase chain reaction analysis of 84 angiogenic factors was performed using mouse-specific angiogenic factors RT2 Profiler PCR Arrays (QIAGEN Inc),
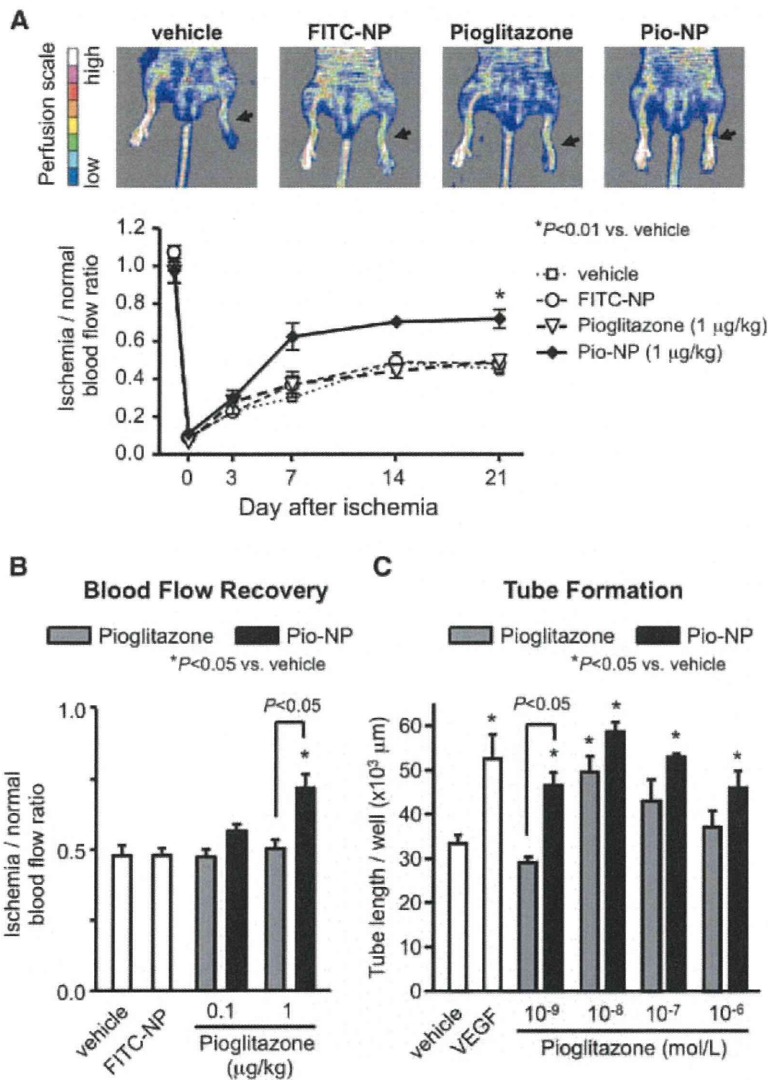
Figure 1. The effects of pioglitazone and pioglitazone-incorporated nanoparticle (Pio-NP) on ischemia-induced neovascularization. **A,** Representative laser Doppler perfusion imaging (LDPI) 21 days after inducing hindlimb ischemia (upper images). The arrow indicates ischemic limb. Quantification of LDPI-derived blood flow recovery. n=6 to 7. *P<0.01 vs no treatment group. The data were compared using 1-way ANOVA followed by Bonferroni multiple comparison tests. **B,** Quantification of LDPI-derived blood flow recovery 21 days after induction of hindlimb ischemia. n=6 to 7. The data were compared using 2-way ANOVA followed by Bonferroni multiple comparison tests. *P<0.05 vs control. **C,** The effects of Pio-NP or pioglitazone on the angiogenic capacity of human endothelial cells in vitro. Quantitative analysis of tube formation (tube length) of 4 independent experiments. The data were compared using 2-way ANOVA followed by Bonferroni multiple comparison tests. *P<0.05 vs control. VEGF indicates vascular endothelial growth factor; FITC, fluorescein isothiocyanate.

according to the manufacturer's protocol. The complete list of the genes analyzed is available online at http://www.sabiosciences.com/rt_pcr_product/HTML/PARN-030A.html. The relative gene expression levels were normalized to the housekeeping gene hypoxanthine phosphoribosyltransferase-1. Data analysis was performed using the ΔΔCt-based fold-change method.

Angiogenesis Assay in Human Umbilical Vein Endothelial Cells

We performed a 2-dimensional Matrigel assay in human umbilical vein endothelial cells. Additional details are provided in the Methods in the online-only Data Supplement.

Western Blot Analysis

The homogenates of the muscle tissues were analyzed for immunoblotting 3 days after inducing hindlimb ischemia. The membrane was incubated with antibodies against phosphorylated Akt, phosphorylated endothelial NO synthase (eNOS), Akt (Cell Signaling, Danvers, MA), and eNOS (Thermo Fisher Scientific Inc).

Statistical Analysis

The data are expressed as the mean±SEM. The statistical analysis was assessed using analysis of variance and multiple comparison tests. *P* values <0.05 were considered to be statistically significant.

Results

Tissue Distribution of PLGA NP

We first examined the distribution of FITC after an injection of either FITC-NP or FITC into ischemic hindlimb muscles in a murine model. FITC fluorescence was detectable for 14 days in the FITC-NP–injected hindlimbs, whereas FITC fluorescence was undetectable at day 7 in FITC only–injected hindlimbs (Figure II in the online-only Data Supplement), suggesting NP-dependent modification of pharmacokinetics as shown in our previous study.[10]

Pio-NP Enhanced Ischemia-Induced Neovascularization

We examined the effect of Pio-NP on blood flow recovery after induction of acute hindlimb ischemia in a murine model using LDPI. Importantly, a single intramuscular injection of Pio-NP containing 1 μg/kg pioglitazone significantly enhanced blood flow recovery in the ischemic limbs, whereas an intramuscular injection of PBS (vehicle), FITC-NP, or 1 μg/kg pioglitazone had no therapeutic effects (Figure 1A and 1B). After injecting pioglitazone or Pio-NP into ischemic hindlimbs, we examined the tissue and serum concentration of pioglitazone at several

Table 1. Tissue and Serum Pioglitazone Concentrations After Intramuscular Injection of Pioglitazone or Pioglitazone-NP

	Time After Injection			
	15 min	1 h	6 h	24 h
Pioglitazone only at 1 μg/kg				
Muscle, ng/g tissue	19±1	ND	ND	ND
Serum, ng/mL	1±1	ND	1±1	ND
Pioglitazone-NP containing 1 μg/kg pioglitazone				
Muscle, ng/g tissue	37±4*	5±2	2±1	ND
Serum, ng/mL	2±1	1±1	2±0	ND

ND indicates not detected (muscle <1 ng/g tissue; serum <1 ng/mL); NP, nanoparticle.

*$P<0.05$ vs pioglitazone.

time points. As shown in Table 1, Pio-NP remained detectable for 6 hours in the muscular tissue compared with pioglitazone alone. The concentration of pioglitazone in the muscular tissue was estimated to be 37±4 ng/g tissue 15 minutes after injecting Pio-NP containing 1 μg/kg pioglitazone and was below the detectable limit ($\approx$1.0 ng/g tissue) after 24 hours. By contrast, pioglitazone was undetectable 1 hour after injecting 1 μg/kg pioglitazone alone (Table 1), suggesting that NP enhanced the accumulation of pioglitazone within the hindlimb tissue.

We then tested the angiogenic activity of pioglitazone in cultured endothelial cells in vitro. Pio-NP induced significant endothelial tube formation in human umbilical vein endothelial cells at 10^{-9} to 10^{-6} mol/L, which was equivalent to the effect induced by VEGF (10 ng/mL; Figure 1C). The induction of endothelial tube formation was significantly enhanced with Pio-NP compared with pioglitazone alone at the same doses, suggesting that NP modified the drug kinetics and efficacy. Pio-NP–induced blood flow recovery was accompanied by a significant increase in the number of CD31-positive endothelial cells surrounding the regenerating myocytes and an increase in number of capillary and arterioles accompanied by α-smooth muscle actin–positive smooth muscle cells 21 days after inducing ischemia (Figure 2).

Pio-NP Enhances Ischemic Neovascularization Through PPAR-γ Activation

We questioned whether Pio-NP–induced neovascularization is dependent solely on PPAR-γ activation. The blood flow recovery by Pio-NP was reversed in mice pretreated with the PPAR-γ antagonist GW9662, suggesting that PPAR-γ activation is critical for Pio-NP–induced blood flow recovery (Figure 3A). Indeed, Pio-NP significantly activated PPAR-γ DNA binding in the nuclear extract from the ischemic hindlimb tissues. Systemic pretreatment with GW9662 again reversed the Pio-NP–induced PPAR-γ activation in the hindlimb tissues (Figure 3B, left). By contrast, an intramuscular injection of Pio-NP in the ischemic limbs did not affect PPAR-γ transcriptional activity in the contralateral nonischemic limbs (Figure 3B, right). The serum levels of glucose, triglyceride, and insulin did not differ between the control group and the oral administration of pioglitazone groups. This result suggests that pioglitazone enhances

ischemic neovascularization independent of blood glucose or insulin, even when administered daily, in the nondiabetic murine model (Table I in the online-only Data Supplement).

## Effect of Pio-NP on Endogenous Angiogenic Factor Expression

PPAR-γ may regulate several genes that contribute to ischemic neovascularization. Three days after inducing ischemia, we examined gene expression in the hindlimb tissues that were treated with Pio-NP. Real-time polymerase chain reaction analysis revealed a significant induction of VEGF-A, VEGF-B, VEGF receptor1/Flt-1, fibroblast growth factor-1 (FGF-1), FGF receptor 3, and platelet/endothelial cell adhesion molecule-1 in the ischemic muscle tissues treated with Pio-NP compared with vehicle-treated ischemic muscle tissues (Table 2).

Effects of Pio-NP on Neovascularization Depends on eNOS

The aforementioned angiogenic growth factors were demonstrated to induce the proliferation of endothelial cells, in
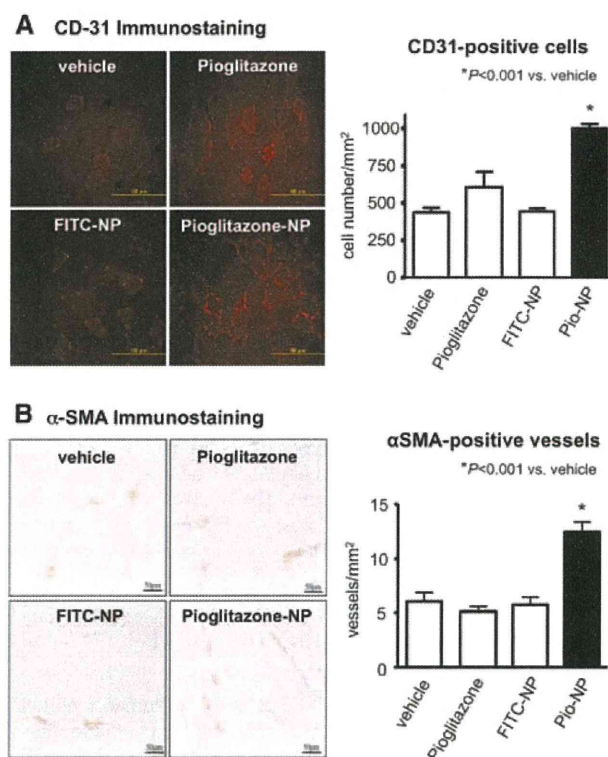
Figure 2. Quantitative analysis of angiogenesis and arteriogenesis. **A,** Immunofluorescent staining of cross sections from ischemic muscle at 21 days after inducing ischemia, stained for the endothelial marker CD31 (red; left). Scale bars, 100 μm. Quantitative analysis of angiogenesis (right; CD31-positive cells per mm²). **B,** Representative micrographs of ischemic muscle sections stained immunohistochemically with antibodies against α-smooth muscle actin (α-SMA) at 21 days after surgery (left). The nuclei were counterstained with hematoxylin. Scale bars, 100 μm. Quantitative analysis of arteriogenesis (right; α-SMA–positive vessels per mm²). The data were compared using 1-way ANOVA followed by Bonferroni multiple comparison tests. *$P<0.001$ vs untreated group. Pio-NP indicates pioglitazone-incorporated nanoparticle.
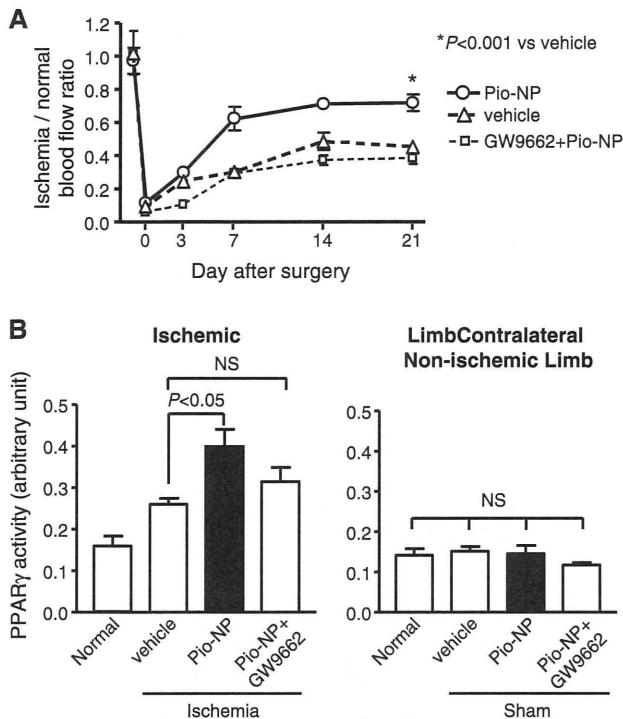
Figure 3. The essential role of peroxisome proliferator–activated receptor-γ (PPAR-γ) in the enhanced ischemia-induced neovascularization induced by pioglitazone-incorporated nanoparticle (Pio-NP). The increased neovascularization induced by Pio-NP was associated with PPAR-γ activity. **A,** Quantification of laser Doppler–derived blood flow recovery after surgery in wild-type mice with or without administration of GW9662, a PPAR-γ inhibitor. **B,** PPAR-γ activation in ischemic muscles 3 days after ischemia. The data were compared using 1-way ANOVA followed by Bonferroni multiple comparison tests. NS indicates not significant.

Table 2. Gene Expression Changes in Pioglitazone-Incorporated Nanoparticle–Treated Ischemic Muscle Tissue Compared With Vehicle-Treated Tissue (Real-Time Polymerase Chain Reaction Array)

Gene Name	Description	Epox/Control Normalized (Increase)	Reference Sequence
FGF-6	Fibroblast growth factor-6	6.04	NM_010204
VEGF-B	Vascular endothelial growth factor-B	3.39	NM_011697
FGF-1	Fibroblast growth factor-1	3.06	NM_010197
—	T-box–1	2.86	NM_011532
PECAM-1	Platelet/endothelial cell adhesion molecule-1	2.61	NM_008816
Agpt2	Angiopoietin-2	2.56	NM_007426
VEGF-A	Vascular endothelial growth factor-A	2.26	NM_009505
EGF	Epidermal growth factor	2.06	NM_010113
Galpha13/AU024132	Guanine nucleotide binding protein, α13	1.96	NM_010303
VEGFR-1/Flt-1	Vascular endothelial growth factor receptor 1	1.90	NM_010228
FGFR-3	Fibroblast growth factor receptor-3	1.74	NM_008010
VEGF-D	Vascular endothelial growth factor-D	1.74	NM_010216

Gene Name	Description	Epox/Control Normalized (Decrease)	Reference Sequence
MK/Mek	Midkine	2.14	NM_010784
TGF-β1	Transforming growth factor-β1	1.78	NM_011577
CINC-2a/Gro2/MIP-2//Mgsa-b/Scyb2	Chemokine (C-X-C motif) ligand-2	1.62	NM_009140
ELF-2/Htk-L/LERK-5	Ephrin-B2	1.60	NM_010111
TSP2/Thbs-2	Thrombospondin-2	1.52	NM_011581

which endothelial NO plays a critical role.[13] PPAR-γ activation induces NO release from endothelial cells, both dependently and independently of eNOS mRNA expression.[14,15] Hence, we examined the role of eNOS expression and its activation in Pio-NP–induced neovascularization in the ischemic hindlimb model. In eNOS^{−/−} mice, femoral artery occlusion induced a relatively severe lesion compared with wild-type mice (data not shown), whereas blood flow recovery determined by LDPI was equivalent in untreated eNOS^{−/−} mice compared with wild-type mice. Importantly, the Pio-NP–induced enhancement was not observed in eNOS^{−/−} mice (Figure 4A), suggesting the critical role of eNOS in the therapeutic effects of Pio-NP. Pio-NP did not affect eNOS mRNA expression (data not shown) and the eNOS protein levels in the ischemic hindlimb tissues in wild-type mice (Figure 4B and 4C). The treatment with Pio-NP significantly increased the phosphorylation of eNOS in ischemic muscles compared with nonischemic control and nontreated ischemic muscles 3 days after treatment (Figure 4C). Pio-NP tended to increase Akt phosphorylation compared with no treatment, although the difference was not statistically significant.

Efficacy of the PLGA NP

Finally, we confirmed the therapeutic advantage of the NP-mediated intramuscular delivery of pioglitazone over

pioglitazone alone or the oral administration of pioglitazone. The daily oral administration of pioglitazone (1 μg/kg per day) did not enhance blood flow recovery. Oral treatment with pioglitazone required as high as 1000 μg/kg per day to significantly enhance blood flow recovery equivalent to Pio-NP (Figure 5A). Finally, a single intramuscular injection of Pio-NP was significantly more effective compared with a single intramuscular injection of pioglitazone alone or daily oral administration of pioglitazone at the same single dose (1 μg/kg) (Figure 5B).

Discussion

There have been controversial results regarding the angiogenic effects of TZDs both in vitro and in vivo.[16] In the present study, we demonstrated that oral treatment with pioglitazone at clinically relevant dose (1000 μg/kg) enhanced blood flow recovery in a hindlimb ischemia model in nondiabetic mice independent of the changes in blood glucose
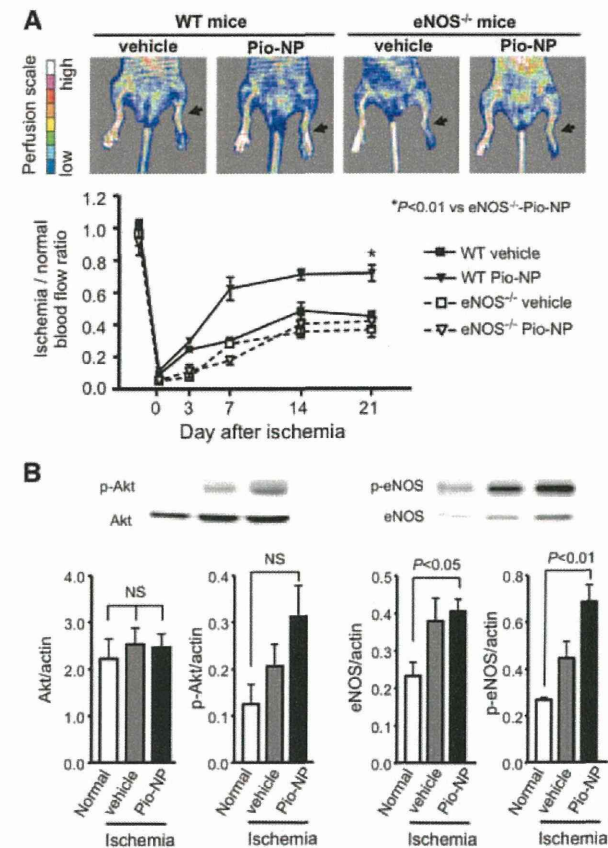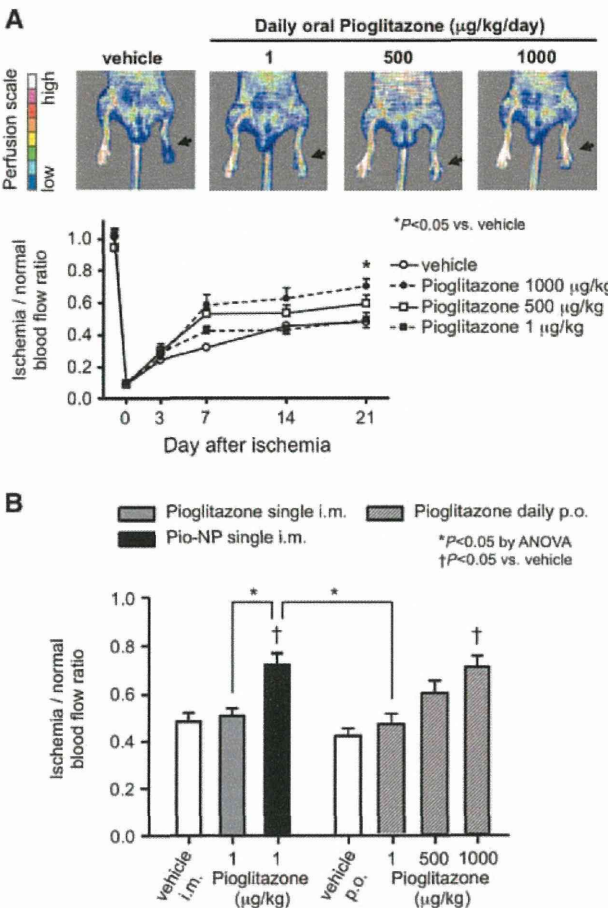
Figure 4. The essential role of endothelial nitric oxide synthase (eNOS) in the enhanced ischemia–induced neovascularization induced by pioglitazone-incorporated nanoparticle (Pio-NP). The increased neovascularization by the Pio-NP was associated with the increased expression of the active forms of eNOS and Akt. **A,** Quantification of laser Doppler–derived blood flow recovery after surgery in wild-type (WT) mice and in eNOS−/− mice. n=5 to 6. *P<0.01 vs no treatment group. **B,** Western blot analysis of phosphorylated Akt and eNOS in ischemic and nonischemic muscles 3 days after ischemia. The quantitative evaluation was expressed as a ratio of phosphorylated Akt, phosphorylated eNOS (p-eNOS), Akt, eNOS to actin. n=4 to 6. The data were compared using 1-way ANOVA followed by Bonferroni multiple comparison tests. NS indicates not significant.

Figure 5. Effects of the daily oral administration of pioglitazone on ischemia-induced neovascularization. **A,** Quantification of laser Doppler perfusion imaging (LDPI)–derived blood flow recovery. n=7 to 8. *P<0.01 vs untreated group. **B,** The effects of single intramuscular injection of pioglitazone- incorporated nanoparticle (Pio-NP) compared with the daily oral administration of pioglitazone 21 days after ischemia. n=7 to 8.

or insulin levels, suggesting that pioglitazone directly acts on vascular cells to enhance ischemia-induced neovascularization. Despite its potential effectiveness, the oral administration of pioglitazone is hampered by its adverse effects, including edema and heart failure.[17] Recently, the potential link between pioglitazone and the risk of bladder cancer has been raised as a concern.[18]
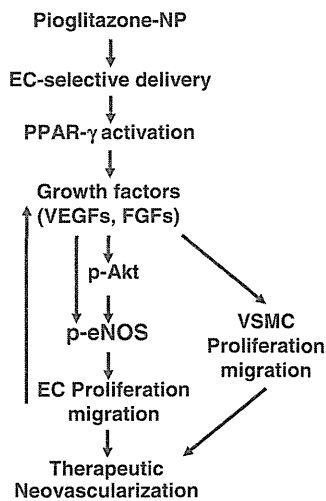
Importantly, we demonstrated that a single intramuscular injection of Pio-NP at as low a concentration as 1 μg/kg had significant therapeutic effects on ischemia-induced neovascularization (Figure 1). The pioglitazone concentrations in the tissue and the serum suggest the local retention of Pio-NP in ischemic skeletal muscles in vivo. The distribution of FITC-NP (Figure II in the online-only Data Supplement) suggests that Pio-NP accumulates in the endothelial cells in the ischemic muscles. In our previous studies,[10,11] we have shown that PLGA NP accumulates preferentially in endothelial cells compared with skeletal muscle cells, relying on clathrin-mediated endocytosis, which may explain the selective distribution in endothelial cells in the muscle tissues. A single intramuscular injection of PLGA NP may cover the therapeutic window for the blood flow recovery in the murine model (≈7 days; eg, Figure 1A), given that we have also demonstrated that PLGA NP (mean diameter =200 nm) gradually undergo hydrolysis over 21 days in a physiological fluid (pH 7.4; 32°C).[10] Importantly, Pio-NP exhibited a significant induction of endothelial tube formation at a wider range of doses (10^−9 to 10^−6 mol/L) compared with pioglitazone alone (Figure 1C), suggesting that PLGA NP–dependent changes in tissue distribution and release kinetics optimized the proangiogenic activity of pioglitazone on endothelial cells. Further studies are needed to clarify the effect of ischemia and the amount of PLGA NP on the mode of endosomal escape, intracellular localization, and drug release kinetics of PLGA NP used in the present study.[19]

PPAR-γ activation appears to be a critical step in therapeutic neovascularization by Pio-NP because we confirmed that Pio-NP induced PPAR-γ DNA binding to the PPAR response element (Figure 3B) and that the PPAR-γ antagonist GW9662 abolished the blood flow recovery by Pio-NP (Figure 3A).

Pioglitazone-NP
↓
EC-selective delivery
↓
PPAR-γ activation
↓
Growth factors
(VEGFs, FGFs)
↓
p-Akt
↓
p-eNOS   VSMC
Proliferation
migration
↓
EC Proliferation
migration
↓
Therapeutic
Neovascularization

Figure 6. Schematic illustration of the effects of pioglitazone nanoparticles. The nanoparticle (NP)–mediated endothelial cell–selective delivery of pioglitazone induces peroxisome proliferator activated receptor-γ (PPAR-γ) activation. PPAR-γ activation with pioglitazone enhances the expression of multiple growth factors in endothelial cells and induced the phosphorylation of Akt and endothelial nitric oxide synthase (eNOS), resulting in enhanced endothelial cell proliferation and migration. Fibroblast growth factors (FGFs) stimulate smooth muscle cell proliferation and migration. The recruitment of endothelial cells and vascular smooth muscle cells (VSMCs) results in arteriogenesis as therapeutic neovascularization. VEGF indicates vascular endothelial growth factor; p-Akt, phosphorylated Akt; p-eNOS; phosphorylated eNOS; EC, endothelial cell.

Ligand-induced activation of PPAR-γ is known to modulate angiogenic factors including VEGF and FGFs via binding to the PPAR response element.[20] Blood flow recovery by Pio-NP was accompanied by arteriogenesis in ischemic hindlimb muscle, which is demonstrated as arterioles with α-smooth muscle actin–positive pericytes. Polymerase chain reaction array revealed that Pio-NP induced multiple genes that are involved in endothelial proliferation and migration (VEGF-A, VEGF-B, VEGF-D, and epidermal growth factor),[21–26] as well as vascular smooth muscle cell migration and proliferation (FGF and Gna13).[27–30] This coordinated induction of endothelial cells and VSMCs is critical for Pio-NP–induced mature arteriogenesis to form functional collaterals.

Recent phase II randomized clinical trials designed to prove the therapeutic neovascularization for ischemic vascular disease by administering exogenous angiogenic growth factors failed to demonstrate the clinical benefits, although each angiogenic growth factor induces angiogenesis (increased capillary density) in preclinical studies.[31,32] Arteriogenesis, defined as the enlargement of preexisting collateral arteries and their remodeling to conductance vessels, is considered to be more effective at inducing blood flow recovery.[33] In the present study, we performed a histological evaluation of the peripheral ischemic muscles and discovered an increased number of endothelial cells (capillaries), as well as smooth muscle cells forming arterioles (Figure 2) along with overall blood flow recovery. These data suggest that neovascularization in the peripheral muscles may induce arteriogenesis in the proximal regions, which remains to be clarified in larger animal models such as rabbits.[11]

eNOS activation appears to be essential for Pio-NP–induced neovascularization, as shown in the experiment using eNOS$^{-/-}$ mice (Figure 4). Several angiogenic factors including VEGF-A, VEGF-B, and FGF are known to activate eNOS phosphorylation in an Akt-dependent and Akt-independent fashion, and the increased endothelium-derived NO in turn mediates the proliferation of endothelial cells,[34–37] which may be a central mechanism of Pio-NP–induced neovascularization (Figure 6). The therapeutic effects afforded by Pio-NP were independent of the improvement in insulin resistance. We demonstrated that the intramuscular injection of Pio-NP did not affect glucose, insulin, or triglyceride levels in the serum. These findings suggest that Pio-NP acted locally on ischemic vascular endothelial cells to induce therapeutic neovascularization.

In conclusion, the NP-mediated endothelial cell–selective delivery of pioglitazone induces functionally mature collaterals through eNOS activation and the expression of multiple endogenous angiogenic growth factors. NP-mediated drug delivery is a novel modality that may advance therapeutic neovascularization over current medical treatment for severe peripheral artery disease, including CLI.

Disclosures
Dr Egashira holds a patent on the results reported in this study. The remaining authors report no conflict of interest.

References
1. Adam DJ, Beard JD, Cleveland T, Bell J, Bradbury AW, Forbes JF, Fowkes FG, Gillepsie I, Ruckley CV, Raab G, Storkey H; BASIL trial participants. Bypass versus angioplasty in severe ischaemia of the leg (BASIL): multicentre, randomised controlled trial. *Lancet.* 2005;366:1925–1934.
2. Hirsch AT, Haskal ZJ, Hertzer NR, et al. ACC/AHA 2005 Practice Guidelines for the management of patients with peripheral arterial disease (lower extremity, renal, mesenteric, and abdominal aortic): a collaborative report from the American Association for Vascular Surgery/ Society for Vascular Surgery, Society for Cardiovascular Angiography and Interventions, Society for Vascular Medicine and Biology, Society of Interventional Radiology, and the ACC/AHA Task Force on Practice Guidelines (Writing Committee to Develop Guidelines for the Management of Patients With Peripheral Arterial Disease): endorsed by the American Association of Cardiovascular and Pulmonary Rehabilitation; National Heart, Lung, and Blood Institute; Society for Vascular Nursing; TransAtlantic Inter-Society Consensus; and Vascular Disease Foundation. *Circulation.* 2006;113:e463–e654.
3. Fukunaga Y, Itoh H, Doi K, Tanaka T, Yamashita J, Chun TH, Inoue M, Masatsugu K, Sawada N, Saito T, Hosoda K, Kook H, Ueda M, Nakao K. Thiazolidinediones, peroxisome proliferator-activated receptor gamma agonists, regulate endothelial cell growth and secretion of vasoactive peptides. *Atherosclerosis.* 2001;158:113–119.
4. Gensch C, Clever YP, Werner C, Hanhoun M, Böhm M, Laufs U. The PPAR-gamma agonist pioglitazone increases neoangiogenesis and prevents apoptosis of endothelial progenitor cells. *Atherosclerosis.* 2007;192:67–74.
5. Murata T, He S, Hangai M, Ishibashi T, Xi XP, Kim S, Hsueh WA, Ryan SJ, Law RE, Hinton DR. Peroxisome proliferator-activated receptor-gamma ligands inhibit choroidal neovascularization. *Invest Ophthalmol Vis Sci.* 2000;41:2309–2317.
6. Chu K, Lee ST, Koo JS, Jung KH, Kim EH, Sinn DI, Kim JM, Ko SY, Kim SJ, Song EC, Kim M, Roh JK. Peroxisome proliferator-activated

receptor-gamma-agonist, rosiglitazone, promotes angiogenesis after focal cerebral ischemia. *Brain Res.* 2006;1093:208–218.

7. Panigrahy D, Singer S, Shen LQ, Butterfield CE, Freedman DA, Chen EJ, Moses MA, Kilroy S, Duensing S, Fletcher C, Fletcher JA, Hlatky L, Hahnfeldt P, Folkman J, Kaipainen A. PPARgamma ligands inhibit primary tumor growth and metastasis by inhibiting angiogenesis. *J Clin Invest.* 2002;110:923–932.

8. Biscetti F, Gaetani E, Flex A, Aprahamian T, Hopkins T, Straface G, Pecorini G, Stigliano E, Smith RC, Angelini F, Castellot JJ Jr, Pola R. Selective activation of peroxisome proliferator-activated receptor (PPAR)alpha and PPAR gamma induces neoangiogenesis through a vascular endothelial growth factor-dependent mechanism. *Diabetes.* 2008;57:1394–1404.

9. Huang PH, Sata M, Nishimatsu H, Sumi M, Hirata Y, Nagai R. Pioglitazone ameliorates endothelial dysfunction and restores ischemia-induced angiogenesis in diabetic mice. *Biomed Pharmacother.* 2008;62:46–52.

10. Kubo M, Egashira K, Inoue T, Koga J, Oda S, Chen L, Nakano K, Matoba T, Kawashima Y, Hara K, Tsujimoto H, Sueishi K, Tominaga R, Sunagawa K. Therapeutic neovascularization by nanotechnology-mediated cell-selective delivery of pitavastatin into the vascular endothelium. *Arterioscler Thromb Vasc Biol.* 2009;29:796–801.

11. Oda S, Nagahama R, Nakano K, Matoba T, Kubo M, Sunagawa K, Tominaga R, Egashira K. Nanoparticle-mediated endothelial cell-selective delivery of pitavastatin induces functional collateral arteries (therapeutic arteriogenesis) in a rabbit model of chronic hind limb ischemia. *J Vasc Surg.* 2010;52:412–420.

12. Kawashima Y, Yamamoto H, Takeuchi H, Hino T, Niwa T. Properties of a peptide containing DL-lactide/glycolide copolymer nanospheres prepared by novel emulsion solvent diffusion methods. *Eur J Pharm Biopharm.* 1998;45:41–48.

13. Lamalice L, Le Boeuf F, Huot J. Endothelial cell migration during angiogenesis. *Circ Res.* 2007;100:782–794.

14. Yuen CY, Wong WT, Tian XY, Wong SL, Lau CW, Yu J, Tomlinson B, Yao X, Huang Y. Telmisartan inhibits vasoconstriction via PPAR?-dependent expression and activation of endothelial nitric oxide synthase. *Cardiovasc Res.* 2011;90:122–129.

15. Calnek DS, Mazzella L, Roser S, Roman J, Hart CM. Peroxisome proliferator-activated receptor gamma ligands increase release of nitric oxide from endothelial cells. *Arterioscler Thromb Vasc Biol.* 2003;23:52–57.

16. Margeli A, Kouraklis G, Theocharis S. Peroxisome proliferator activated receptor-gamma (PPAR-gamma) ligands and angiogenesis. *Angiogenesis.* 2003;6:165–169.

17. Guan Y, Hao C, Cha DR, Rao R, Lu W, Kohan DE, Magnuson MA, Redha R, Zhang Y, Breyer MD. Thiazolidinediones expand body fluid volume through PPARgamma stimulation of ENaC-mediated renal salt absorption. *Nat Med.* 2005;11:861–866.

18. Tseng CH. Pioglitazone and bladder cancer in human studies: is it diabetes itself, diabetes drugs, flawed analyses or different ethnicities? *J Formos Med Assoc.* 2012;111:123–131.

19. Danhier F, Ansorena E, Silva JM, Coco R, Le Breton A, Préat V. PLGA-based nanoparticles: An overview of biomedical applications. *J Control Release.* 2012;161:505–522.

20. Cho DH, Choi YJ, Jo SA, Jo I. Nitric oxide production and regulation of endothelial nitric-oxide synthase phosphorylation by prolonged treatment with troglitazone: evidence for involvement of peroxisome proliferator-activated receptor (PPAR) gamma-dependent and PPARgamma-independent signaling pathways. *J Biol Chem.* 2004;279:2499–2506.

21. Silvestre JS, Tamarat R, Ebrahimian TG, Le-Roux A, Clergue M, Emmanuel F, Duriez M, Schwartz B, Branellec D, Lévy BI. Vascular endothelial growth factor-B promotes in vivo angiogenesis. *Circ Res.* 2003;93:114–123.

22. Im E, Kazlauskas A. Regulating angiogenesis at the level of PtdIns-4,5-P2. *EMBO J.* 2006;25:2075–2082.

23. Matsumoto T, Claesson-Welsh L. VEGF receptor signal transduction. *Sci STKE.* 2001;2001:re21.

24. Rahimi N. VEGFR-1 and VEGFR-2: two non-identical twins with a unique physiognomy. *Front Biosci.* 2006;11:818–829.

25. Normanno N, De Luca A, Bianco C, Strizzi L, Mancino M, Maiello MR, Carotenuto A, De Feo G, Caponigro F, Salomon DS. Epidermal growth factor receptor (EGFR) signaling in cancer. *Gene.* 2006;366:2–16.

26. Jauhiainen S, Häkkinen SK, Toivanen PI, Heinonen SE, Jyrkkänen HK, Kansanen E, Leinonen H, Levonen AL, Ylä-Herttuala S. Vascular endothelial growth factor (VEGF)-D stimulates VEGF-A, stanniocalcin-1, and neuropilin-2 and has potent angiogenic effects. *Arterioscler Thromb Vasc Biol.* 2011;31:1617–1624.

27. Doukas J, Blease K, Craig D, Ma C, Chandler LA, Sosnowski BA, Pierce GF. Delivery of FGF genes to wound repair cells enhances arteriogenesis and myogenesis in skeletal muscle. *Mol Ther.* 2002;5:517–527.

28. Ghiselli G, Chen J, Kaou M, Hallak H, Rubin R. Ethanol inhibits fibroblast growth factor-induced proliferation of aortic smooth muscle cells. *Arterioscler Thromb Vasc Biol.* 2003;23:1808–1813.

29. Offermanns S, Mancino V, Revel JP, Simon MI. Vascular system defects and impaired cell chemokinesis as a result of Galpha13 deficiency. *Science.* 1997;275:533–536.

30. Boilly B, Vercoutter-Edouart AS, Hondermarck H, Nurcombe V, Le Bourhis X. FGF signals for cell proliferation and migration through different pathways. *Cytokine Growth Factor Rev.* 2000;11:295–302.

31. Losordo DW, Dimmeler S. Therapeutic angiogenesis and vasculogenesis for ischemic disease. Part I: angiogenic cytokines. *Circulation.* 2004;109:2487–2491.

32. van Royen N, Piek JJ, Schaper W, Fulton WF. A critical review of clinical arteriogenesis research. *J Am Coll Cardiol.* 2009;55:17–25.

33. Schaper W, Scholz D. Factors regulating arteriogenesis. *Arterioscler Thromb Vasc Biol.* 2003;23:1143–1151.

34. Hayakawa H, Hirata Y, Kakoki M, Suzuki Y, Nishimatsu H, Nagata D, Suzuki E, Kikuchi K, Nagano T, Kangawa K, Matsuo H, Sugimoto T, Omata M. Role of nitric oxide-cGMP pathway in adrenomedullin-induced vasodilation in the rat. *Hypertension.* 1999;33:689–693.

35. Murohara T, Asahara T, Silver M, Bauters C, Masuda H, Kalka C, Kearney M, Chen D, Symes JF, Fishman MC, Huang PL, Isner JM. Nitric oxide synthase modulates angiogenesis in response to tissue ischemia. *J Clin Invest.* 1998;101:2567–2578.

36. Ziche M, Morbidelli L, Choudhuri R, Zhang HT, Donnini S, Granger HJ, Bicknell R. Nitric oxide synthase lies downstream from vascular endothelial growth factor-induced but not basic fibroblast growth factor-induced angiogenesis. *J Clin Invest.* 1997;99:2625–2634.

37. Duval M, Le Boeuf F, Huot J, Gratton JP. Src-mediated phosphorylation of Hsp90 in response to vascular endothelial growth factor (VEGF) is required for VEGF receptor-2 signaling to endothelial NO synthase. *Mol Biol Cell.* 2007;18:4659–4668.

Supplementary Figure Legends

Supplementary Figure I. Animal experimental protocols.

In protocol 1, the treatment groups received intramuscular injections of FITC-NP (0.9 mg/100 μl PLGA; NP group), pioglitazone at 0.0025, 0.025 μg/100 μl (1 μg/kg; pioglitazone group), or pioglitazone-NP (0.067, 0.67 μg/100 μl PLGA containing 0.0025, 0.025 μg pioglitazone) into the left femoral and thigh muscles using a 27-gauge needle. In protocol 2, the effects of the intramuscular injections of pioglitazone-NP were examined in wild-type mice administered GW9662 (PPAR-γ antagonist) (Sigma). In protocol 3, the effects of the intramuscular injections of pioglitazone-NP were examined in endothelial nitric oxide synthase (eNOS) $^{-/-}$ mice. WT mice or eNOS$^{-/-}$ mice received single intramuscular injections of pioglitazone-NP at doses of 1 μg/kg immediately after inducing ischemia. In protocol 4, immediately after inducing ischemia, the animals were randomly divided into three groups; three other groups received a systemic daily oral administration of pioglitazone at doses of 1, 500 and 1000 μg/kg dissolved in 0.5% carboxymethyl cellulose by gavage from the day of surgery until the mice were euthanized on day 21.

Supplementary Figure II. Cellular distribution of NP in ischemic muscles.

A, Representative light (upper panels) and fluorescent (lower panels) stereomicrographs of the gastrocnemius muscles isolated from a control, non-ischemic hindlimb and those from an ischemic hindlimb injected with FITC-NP or FITC alone. B, Quantitative analysis of the magnitude of intracellular FITC fluorescence signals in the gastrocnemius muscles are shown. The data were compared using two-way ANOVA followed by Bonferroni's multiple comparison tests. *$p<0.05$ versus control condition. [†]$p<0.05$ versus FITC. C, Immunofluorescent staining of cross-sections from ischemic muscle 3 days after a FITC-NP or FITC only injection stained with the endothelial marker CD31 (red). Scale bars: 100 μm.
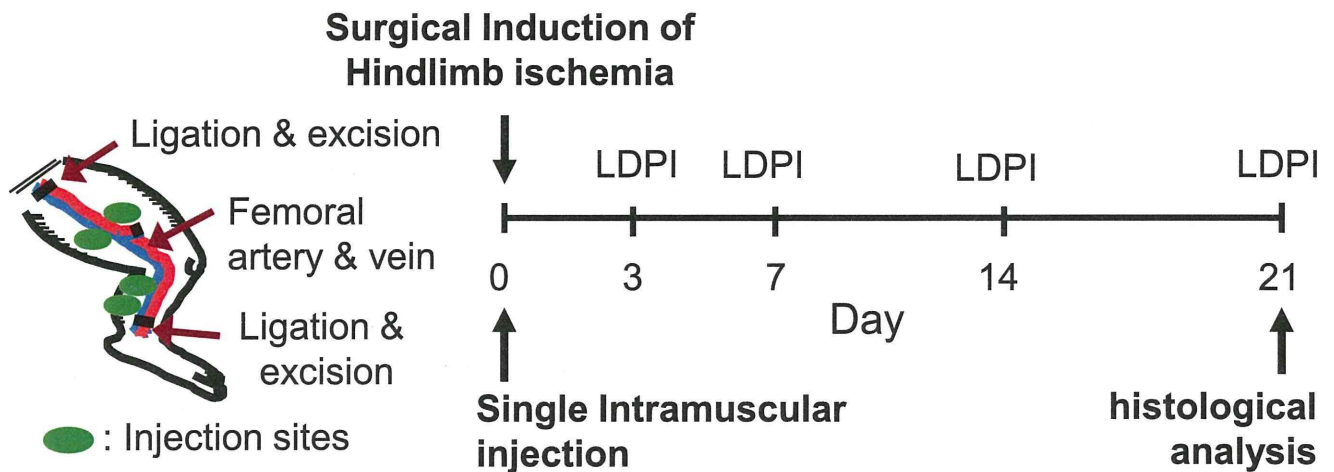
Supplemental Table I. Serum concentration of glucose, triglyceride and insulin at 3

weeks after daily oral administration of pioglitazone

Oral Pioglitazone (mg/kg/day)	Body Weight (g)	Serum Glucose (mg/dL)	Serum Triglyceride (mg/dL)	Serum Insulin (μIU/mL)
0	24.4±0.6	303±33	39±2	ND
1	24.5±1.0	272±23	55±11	ND
500	24.4±1.2	309±114	60±12	ND
1000	23.6±0.9	280±48	63±10	ND

ND: not detected (<0.3 μIU/mL)

The data are shown as the mean±SEM (n=2-5 each).
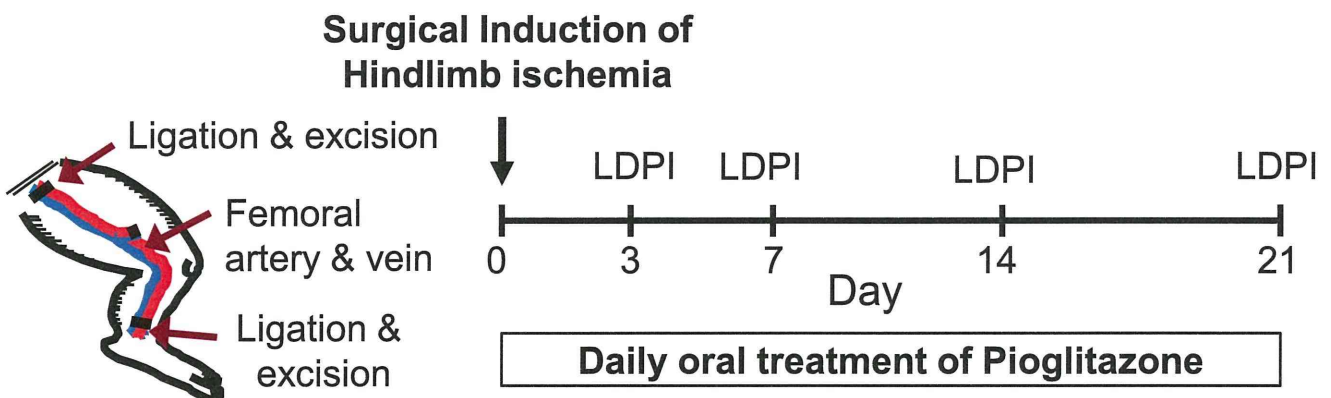
Supplementary Figure I Nagahama R *et al.*

Surgical Induction of Hindlimb ischemia

Ligation & excision

Femoral artery & vein

Ligation & excision

🟢 : Injection sites

LDPI   LDPI   LDPI   LDPI

0   3   7   14   21

Day

Single Intramuscular injection

histological analysis

Protocol 1.
•vehicle
•FITC-NP (control NP)
•Pioglitazone (0.1, 1 µg/kg)
•Pio-NP (0.1, 1 µg/kg as Pioglitazone)

Protocol 2.
•vehicle
•Pio-NP (1 µg/kg as Pioglitazone)
•GW9662 i.p. + Pio-NP (1 µg/kg as Pioglitazone)

Protocol 3.
•WT mice, vehicle
•WT mice, Pio-NP (1 µg/kg as Pioglitazone)
•eNOS-/- mice, vehicle
•eNOS-/- mice, Pio-NP (1 µg/kg as Pioglitazone)

Surgical Induction of Hindlimb ischemia

Ligation & excision

Femoral artery & vein

Ligation & excision

LDPI   LDPI   LDPI   LDPI

0   3   7   14   21

Day

Daily oral treatment of Pioglitazone

Protocol 4.
•Vehicle
•Pioglitazone (1, 500, 1000 µg/kg)

Supplementary Figure Ⅱ Nagahama R *et al.*

A

No Tx FITC only FITC-NP

Light

Fluorescence

3 3 7 14 21

Day after injection

B

☐ FITC only
■ FITC NP

*P<0.05 vs. No Tx
†P<0.05 vs. FITC

Fluorescent intensity (arbitrary units)

50
40
30
20
10
0

0 3 7 14 21

Day after injection

C

FITC only

FITC-NP

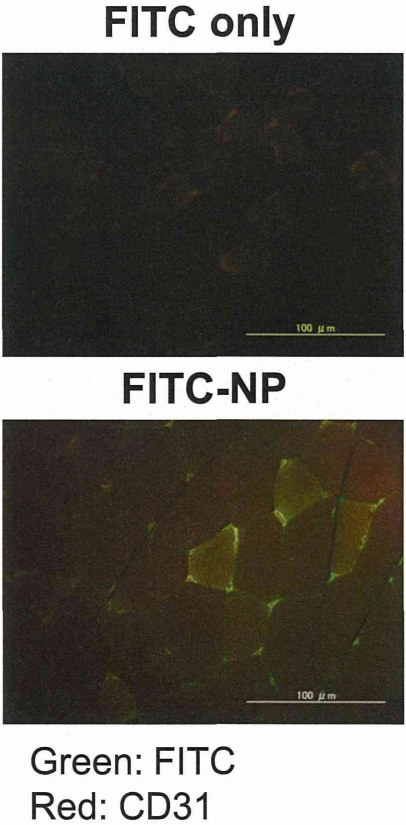Green: FITC
Red: CD31
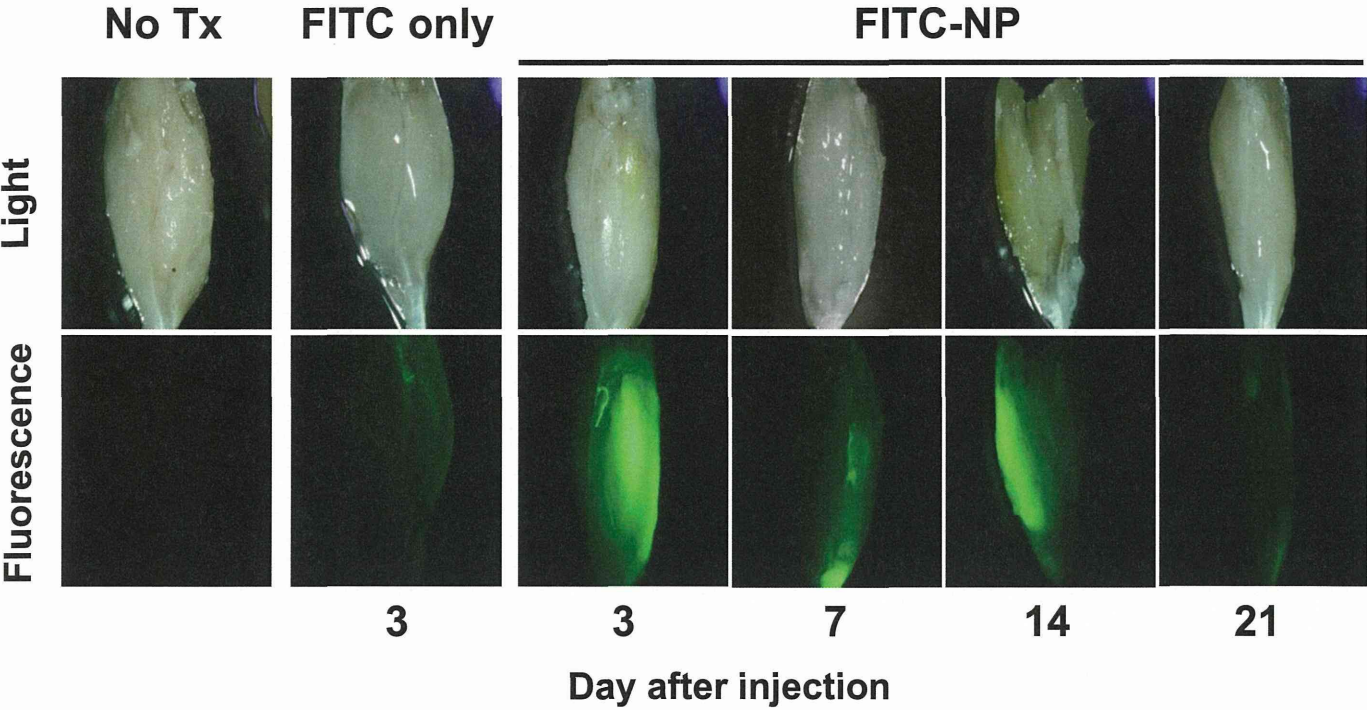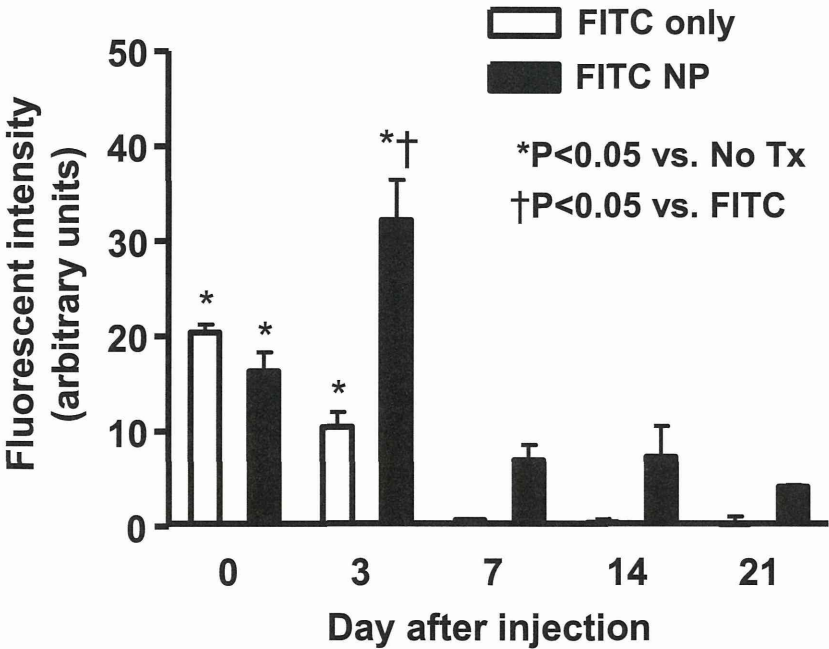
Original Article

Pitavastatin-Incorporated Nanoparticle-Eluting Stents Attenuate In-Stent Stenosis without Delayed Endothelial Healing Effects in a Porcine Coronary Artery Model

Noriaki Tsukie[1], Kaku Nakano[1], Tetsuya Matoba[1], Seigo Masuda[1], Eiko Iwata[1], Miho Miyagawa[1], Gang Zhao[3], Wei Meng[3], Junji Kishimoto[2], Kenji Sunagawa[1] and Kensuke Egashira[1]

[1] Department of Cardiovascular Medicine, Graduate School of Medical Sciences, Kyushu University, Fukuoka, Japan
[2] Digital Medicine Initiative, Graduate School of Medical Sciences, Kyushu University, Fukuoka, Japan
[3] Department of Cardiovascular Medicine, 6th People's Hospital, Shanghai Jiatong University, Shanghai, China

Aim: The use of currently marketed drug-eluting stents presents safety concerns including increased late thrombosis, which is thought to result mainly from delayed endothelial healing effects (impaired re-endothelialization resulting in abnormal inflammation and fibrin deposition). We recently developed a bioabsorbable polymeric nanoparticle (NP)-eluting stent using a novel cationic electrodeposition technology. Statins are known to inhibit the proliferation of vascular smooth muscle cells (VSMC) and to promote vascular healing. We therefore hypothesized that statin-incorporated NP-eluting stents would attenuate in-stent stenosis without delayed endothelial healing effects.
Methods: Among six marketed statins, pitavastatin (Pitava) was found to have the most potent effects on VSMC proliferation and endothelial regeneration *in vitro*. We thus formulated a Pitava-NP-eluting stent (20 μg Pitava per stent).
Results: In a pig coronary artery model, Pitava-NP-eluting stents attenuated in-stent stenosis as effectively as polymer-coated sirolimus-eluting stents (SES). At SES sites, delayed endothelial healing effects were noted, whereas no such effects were observed in Pitava-NP-eluting stent sites.
Conclusion: Pitava-NP-eluting stents attenuated in-stent stenosis as effectively as SES without the delayed endothelial healing effects of SES in a porcine coronary artery model. This nanotechnology platform could be developed into a safer and more effective device in the future.

J Atheroscler Thromb, 2013; 20:32-45.

Key words; Statin, Nanotechnology, Drug delivery system, Signal transduction

Introduction

Increased risk of late in-stent thrombosis resulting in acute coronary syndrome (unstable angina, acute myocardial infarction and death) after the use of drug-eluting stent (DES) devices has become a major safety concern[1-3]. These adverse effects are thought to result mainly from the anti-healing effects of the drugs (sirolimus and paclitaxel) on endothelial cells, leading to impaired re-endothelialization, excessive inflammation, proliferation and fibrin deposition[4-6]. These "anti-healing" drugs are used in most newer generation DESs, leading to continued safety concerns; therefore, the cellular and/or molecular targeting of both VSMC proliferation and re-endothelialization is an essential requirement for the development of more efficient and safer DESs. The use of an anti-healing approach that accelerates re-endothelialization, protects against thrombosis and decreases restenosis is warranted. Comparator analysis of endothelial cell coverage in four marketed polymeric DESs in rabbits has demonstrated a disparity in arterial healing; notably, all DESs examined showed a lack of endothelial anticoagulant function, independent of endothelial coverage[7].

We hypothesized that HMG-CoA reductase inhibitors, so-called statins, are appropriate candidate drugs for the anti-healing strategy because the vascular endothelium is a major target for the pleiotropic (non-LDL-related) vasculoprotective effects of statins[8]. In cell culture experiments *in vitro*, statins reportedly promoted endothelial regeneration and inhibited VSMC proliferation and tissue factor expression[8, 9]. Systemic administration of statins has been reported to inhibit balloon injury-induced and in-stent neointima formation in non-hypercholesterolemic animals. Most of these beneficial effects of statins on neointima formation in animals, however, were observed following daily administration of high doses[8, 10] (rosuvastatin 20 mg/kg per day[11], pitavastatin 40 mg/kg per day[12], simvastatin 40 mg/kg per day[13]); this may lead to serious adverse side effects in a clinical setting. Furthermore, it has been reported that the use of polymer-coated stents with atorvastatin or cerivastatin has no consistent effect on neointima formation in a porcine in-stent stenosis model[14, 15]. Randomized clinical studies in humans have reported no definite effects of statins within the clinical dose range with respect to indices of restenosis after coronary balloon angioplasty[16-19] or coronary stenting[20, 21]; therefore, preventing in-stent restenosis via statin-mediated "anti-healing" effects requires an efficient local drug delivery system.

To overcome this problem, we recently introduced nanoparticles (NP) formulated from the bioabsorbable polymer poly(DL-lactide-co-glycolide) (PLGA) and succeeded in formulating an NP-eluting stent by a cationic electrodeposition coating technology[22]. Therefore, we hypothesized that statin-NP-eluting stents could be an innovative therapeutic "anti-healing" strategy for treating in-stent stenosis *in vivo*.

Materials and Methods

Statins (simvastatin, pitavastatin, atorvastatin, rosuvastatin, fluvastatin, and pravastatin) were purchased, extracted from products, and purified.

Human Coronary Artery Smooth Muscle Cell Proliferation

Human coronary artery smooth muscle cells (SMC) were cultured as previously described[22, 23] and plated into 96-well culture plates at 1×10^4 cells per well in SMGM2. Proliferation was stimulated by adding human PDGF at 10 ng/mL (Sigma, Tokyo, Japan) or 10% FBS to each well. Either vehicle alone or several concentrations of statins, sirolimus, or paclitaxel were added to the well. Cellular proliferation responses

were determined by evaluating the 5'-bromo-2'-deoxyuridine (BrdU) incorporation rate and/or by a cell counting method, as previously described[22, 23].

Human Endothelial Cell Scratch Motility Assay

A scratch motility assay using human umbilical vein endothelial cells (HUVEC) was performed to assess the re-endothelialization response following endothelial denudation. HUVECs were seeded in collagen I-coated 24-well plates at a density of 2×10^4 cells per well and grown to confluence with EGM2. The monolayers were wounded with a pipet tip, washed with PBS twice, photographed and incubated at 37°C with EBM containing 0.5% BSA containing $VEGF_{165}$ (10 ng/mL, R & D) in the presence or absence of statins, sirolimus, or paclitaxel. After five hours, cells were photographed, and the number of cells that had migrated into the wounded area was counted.

Western Blot Analysis

Human aortic endothelial cells (HAEC) were cultured to confluence in 3 cm dishes and rendered quiescent for 24 hours before stimulation with 1 U/mL thrombin (Sigma). Sirolimus, paclitaxel (both Sigma), and pitavastatin were added to the cells one hour before thrombin (1 U/mL) stimulation. Tissue factor protein expression was determined by Western blot analysis. In another set of experiments, sirolimus was added to HAEC and effects of pitavastatin on sirolimus-induced changes in endothelial nitric oxide synthase (eNOS) and protein kinase B (Akt) protein were examined.

Cell extracts (20 μg) were resolved on 10% reducing SDS-PAGE gels and blotted onto nitrocellulose membranes (Bio-Rad, Hercules, CA). Antibodies against human tissue factor (Calbiochem), phosphorylated-Akt (ser473), phosphorylated-eNOS (ser1177), Akt (Cell Signaling), eNOS (Affinity BioReagents) were used. Immune complexes were visualized with horseradish peroxidase-conjugated secondary antibodies (Pierce, Rockford, IL) using the ECL Plus system (Amersham Biosciences) and were detected with the ECL Detection Kit (Amersham). Blots were normalized against GAPDH expression (Sigma).

Preparation of Cationic PLGA Nanoparticles (NP) with Surface Modification with Chitosan

A lactide/glycolide copolymer (PLGA) with an average molecular weight of 20,000 and a lactide to glycolide copolymer ratio of 75:25 (PLGA7520; Wako Pure Chemical Industries, Osaka, Japan) was used as wall material for the NPs because the bioabsorption

half-life of this product is two weeks in rat tissue (manufacturer's instructions). PLGA NPs incorporated with the fluorescent marker fluorescein isothiocyanate (FITC; Dojindo laboratories, Kumamoto, Japan) or with pitavastatin were prepared by a previously reported emulsion solvent diffusion method in purified water[22]. FITC- and pitavastatin-loaded PLGA NPs contained 5.0% (w/v) FITC and 6.5% (w/v) pitavastatin, respectively, and were preserved as freeze-dried material. The mean particle size was analyzed by the light scattering method (Microtrack UPA150; Nikkiso, Tokyo, Japan). The average diameter of the PLGA NPs was 226 ± 29 nm. The surface charge (zeta potential) was also analyzed by Zetasizer Nano (Sysmex, Hyogo, Japan) and was found to be cationic ($+36$ mV at pH 4.4).

Preparation of NP-Eluting Stents by Cationic Electrodeposition Coating Technology

The 15 mm-long stainless-steel, balloon-expandable stents (Multilink) were ultrasonically cleaned in acetone, ethanol, and demineralized water. The cationic electrodeposited coating was prepared on cathodic stents in NP solution at a concentration of 5 g/L in distilled water with a current maintained between 2.0 and 10.0 mA by a direct current power supply (DC power supply; Nippon Stabilizer Co, Tokyo, Japan) for different periods under sterile conditions.28, 31 The coated stents were then rinsed with demineralized water and dried under a vacuum overnight. This electrodeposition coating procedure produced a coating of approximately 367 ± 77 μg of the PLGA NPs per stent and 20 ± 4 μg of pitavastatin per stent ($n = 12$). The surfaces of some NP-coating stents were examined with scanning electron microscopy (JXM8600; JEOL, Tokyo, Japan), and it was confirmed that the NPs were structurally intact and cohesive[22].

Analysis of Endothelial Surface Coverage by en Face Scanning Electron Microscopy

For evaluation of endothelial coverage, stents were excised seven days after implantation. The stented arteries were fixed *in situ* with 10% neutral-buffered formalin after perfusion with lactated Ringer's solution to remove blood. The samples were further fixed by immersion and then bisected longitudinally with one half processed for scanning electron microscopy (SEM).

Composites of serial en face SEM images acquired at low power ($\times 15$ magnification) were digitally assembled to provide a complete view of the entire luminal stent surface. The images were further enlarged ($\times 200$ magnification), allowing direct visualization of endothelial cells. The extent of endothelial surface coverage above and between stent struts was traced and measured by morphometry software. The results are expressed as a percentage of the total surface area above or between struts or the total and percentage area lacking coverage at each repeated crown along the longitudinal axis from the proximal to the distal orientation. Endothelial cells were identified as sheets of spindle- or polygonal-shaped monolayers in close apposition, a distinguishing feature from other cell types in en face preparations[24]. By contrast, intimal smooth muscle cells showed elongated processes and were generally stacked in disorganized or haphazard layers[24]. Other adherent cells present on stent surfaces included platelets, characteristically 1 to 2 μm in size with an irregular discoid appearance, and inflammatory cells, which were round and varied from 7 to 10 μm in diameter with a ruffled surface. Struts uncovered by endothelium were completely bare or contained thrombi consisting of focal platelet and fibrin aggregates intermixed with red blood cells and inflammatory cells.

Measurements of Pitavastatin Concentration in Serum and Arterial Tissue

Concentrations of pitavastatin in serum and stented arterial tissue were measured at predetermined time points using a column-switching high performance liquid chromatography (HPLC) system as previously reported[25]. Briefly, the column-switching HPLC system consists of two LC-10AD pumps, a SIL-10A auto-sampler, a CTO-10A column oven, a six-port column-switching valve, and an SPD-10A UV-detector (all from Shimadzu, Kyoto, Japan). The column temperature was maintained at 40℃. Pre-prepared serum or tissue homogenate sample solutions were injected from the auto-sampler into the HPLC system, and statin in the sample solutions was detected at 250 nm with a UV detector. The detected peak area was measured with Lc solution software (Shimadzu, Kyoto, Japan).

Animal Preparation and Stent Implantation

All *in vivo* experiments were reviewed and approved by the Committee on Ethics in Animal Experiments, Kyushu University Faculty of Medicine, according to the Guidelines of the American Physiological Society.

Domestic male pigs (Kyudo, Tosu, Japan; aged 2 to 3 months and weighing 25 to 30 kg) received orally aspirin (330 mg/day) and ticlopidine (200 mg/day) until euthanasia from 3 days before stent implantation

Table 1. Inhibitory effects of 6 commercially available statins on proliferation of human coronary artery smooth muscle cells

	IC_{50} values (nmol/L)	efficacy ratio	95% Wald confidence intervals	p value
pitavastatin	193	1	–	–
fluvastatin	836	0.230	0.119, 0.446	<0.001
atorvastatin	2512	0.077	0.039, 0.150	<0.001
simvastatin	3951	0.049	0.023, 0.104	<0.001
rosuvastatin	Not calculated	Not calculated	Not calculated	Not calculated
pravastatin	Not calculated	Not calculated	Not calculated	Not calculated

$n = 6$ each. p values versus pitavastatin by Wald tests in 4-parameter logistic regression model.

procedure. Animals were anesthetized with ketamine hydrochloride (15 mg/kg, IM) and pentobarbital (20 mg/kg, IV). They were then intubated and mechanically ventilated with room air. A preshaped Judkins catheter was inserted into the carotid artery and advanced into the orifice of the left coronary artery. After systemic heparinization (100 IU/kg) and intracoronary administration of nitroglycerin, coronary angiography of the left coronary artery was performed with the use of contrast media (iopamidol 370) in a left oblique view with the angiography system (Toshiba Medical, Tokyo, Japan).

Animals were divided into groups, which underwent deployment of either non-coated bare metal stents (1 week: $n=3$, 4 weeks: $n=12$), FITC-incorporated NP-eluting stents (4 weeks: $n=12$), pitavastatin-incorporated NP-eluting stents (1 week: $n=3$, 4 weeks: $n=12$), or sirolimus-eluting stents (Cypher; 3 mm × 15 mm) (1 week: $n=3$, 4 weeks: $n=12$) in the left anterior descending (LAD) or the left circumflex (LCx) coronary arteries. After arterial blood samples were taken, animals were given a lethal dose of anesthesia after 1 or 4 weeks, and the stented arterial sites and contralateral non-stented sites were excised for biochemical, immunohistochemical, and morphometric analyses.

As another set of experiments, animals were treated with intracoronary administration of pitava-NP at 300 μg (a similar dose to that coated on pitavastatin-NP eluting stent, 4 weeks: $n=6$) and 3000 μg (10x dose coated on pitavastatin-NP eluting stent, 4 weeks: $n=6$) containing 20 and 200 μg pitavastatin, respectively, immediately after deployment of bare metal stents. Pitava-NPs were diluted with 10 mL saline. Intracoronary administration of 10 mL saline was used as a control experiment (4 weeks: $n=5$).

A segment with a mean coronary diameter of 2.5 mm was selected by using quantitative coronary angiography with a stent-to-artery ratio of approximately

1.1 : 1.2. A balloon catheter mounted with a stent was then advanced to the pre-selected coronary segments for deployment over a standard guide-wire. The balloon catheter was inflated at 15 atm for 60 seconds once and was then slowly withdrawn, leaving the stent in place.

Quantitative coronary angiography (Toshiba Medical, Tokyo, Japan) was performed before, immediately after, and 4 weeks after stent implantation to examine the coronary arterial diameter at stented and non-stented sites. The image of a Judkins catheter was used as reference diameter. Arterial pressure, heart rate, and ECG were continuously monitored and recorded on a recorder.

Histopathological Study

Four weeks after the coronary angiographic study, animals were euthanized with a lethal dose of sodium pentobarbital (40 mg/kg intravenously), and histological analysis was performed. The left coronary artery was perfused with 10% buffered formalin at 120 mmHg and fixed for 24 hours. The stented artery segments were isolated and processed as described previously[26]. The segment was divided into two parts at the center of the stent and then embedded in methyl methacrylate mixed with n-butyl methacrylate to allow for sectioning through the metal stent struts. Serial sections were stained with elastica van Gieson and hematoxylin-eosin (HE). The neointimal area, the area within the internal elastic lamina (IEL), and the lumen area were measured by computerized morphometry, which was carried out by a single observer who was blinded to the experimental protocol. All images were captured by an Olympus microscope equipped with a digital camera (HC-2500) and were analyzed using Adobe Photoshop 6.0 and Scion Image 1.62 software. The injury, inflammation, fibrin, hemorrhage and re-endothelialization scores were determined at each strut site, and mean values were calculated for each stented segment.

Statistical Analysis

Data are expressed as the means ± SE. Statistical analysis of differences between two groups was performed with the unpaired *t*-test, and differences among groups were analyzed using ANOVA and multiple comparison tests.

Efficacy ratios (IC$_{50}$ values) of the statins were tested using Wald tests in a four-parameter logistic regression model. Point estimates and Wald 95% confidence intervals for efficacy ratios were calculated. Statistical calculations were performed with SAS preclinical package software version 9.1.3 (SAS Institute Inc., Japan, Tokyo). *P* values < 0.05 were considered significant.

Results

Effects of Statins on Human Coronary Artery Smooth Muscle Cell Proliferation and Endothelial Cell Scratch Motility Assay

To incorporate statins into the NP-eluting stent design, the effects of statins were compared. In the human CASMC proliferation assay (% inhibition of BrdU index), hydrophilic statins (rosuvastatin and pravastatin) had no effects on PDGF-induced proliferation; thus, calculation of the IC$_{50}$ value was impossible for those statins (**Table 1**). By contrast, the other four statins showed concentration-dependent inhibition. The IC$_{50}$ values of the four statins are shown in **Table 1**, which indicates that the value for pitavastatin is lowest.

In the human endothelial cell scratch motility assay (re-endothelialization *in vitro*), only pitavastatin increased the re-endothelialization response following scratch injury; the other five statins showed no such effects (**Fig. 1**). In addition, there was no difference in the re-endothelialization response among the five statins.

Effects of Pitavastatin, Sirolimus, and Paclitaxel on Human Coronary Artery Smooth Muscle Cell Proliferation, Endothelial Cell Scratch Motility Assay, and Tissue Factor Expression in Human Endothelial Cells

To incorporate pitavastatin into the NP-eluting stent design, the effects of pitavastatin were then compared with those of sirolimus and paclitaxel. All three drugs inhibited human CASMC proliferation (**Fig. 2**). In the human endothelial cell scratch motility assay, sirolimus did not affect the re-endothelialization response, whereas the response was significantly delayed in paclitaxel-treated endothelial cells (**Fig. 1**).

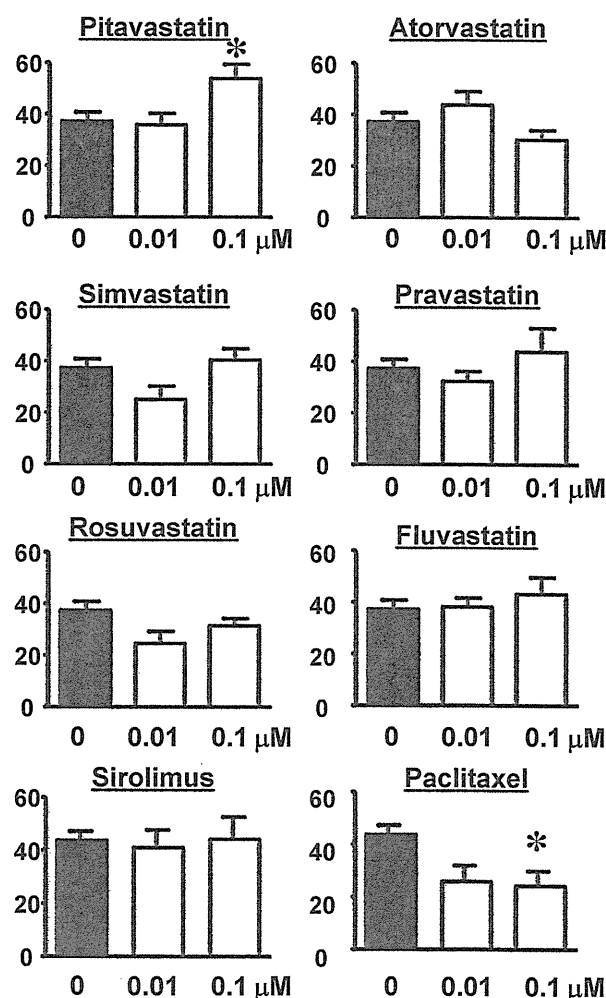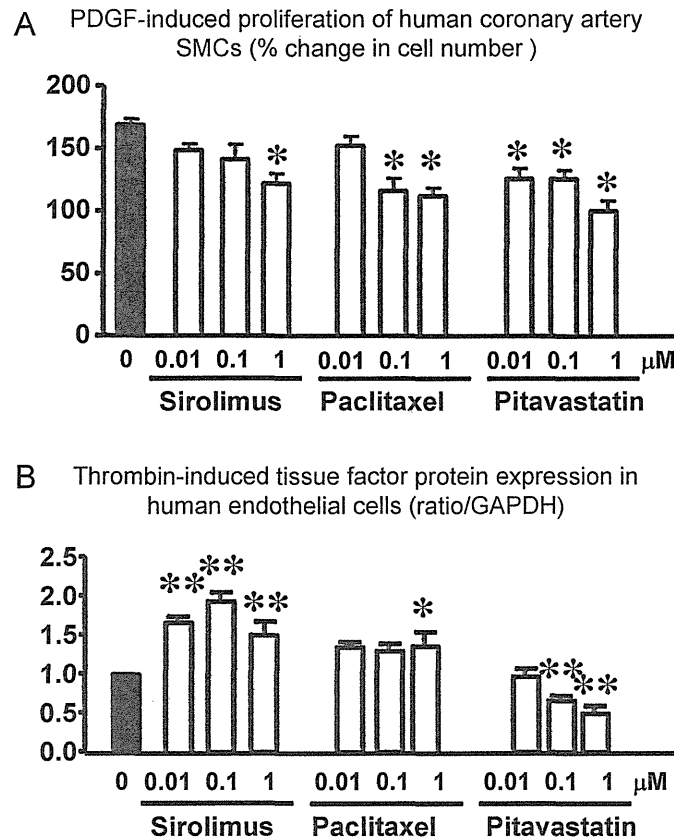Because tissue factor has a primary role in stent

Fig. 1. Human umbilical vein endothelial cell scratch motility assay *in vitro*. Vertical axis denotes the number of migrated cells into the scratched area. *$p < 0.05$ vs no treatment by one-way ANOVA followed with Dunnett's multiple comparison test ($n = 6$-8 each).

thrombosis, its protein expression was examined in human endothelial cells. As previously reported by others[27], both sirolimus and paclitaxel enhanced the thrombin-induced tissue factor expression (**Fig. 2**). By contrast, pitavastatin inhibited tissue factor expression (**Fig. 2**).

Effects of Pitavastatin on Sirolimus-Induced Down Regulation of eNOS in Human Endothelial Cells

Sirolimus down regulated phosphorylated-eNOS and decreased phosphorylated Akt (a representative down stream signal of eNOS), while sirolimus had no effects on eNOS and Akt protein expression (**Fig. 3**).

A PDGF-induced proliferation of human coronary artery
SMCs (% change in cell number)

B Thrombin-induced tissue factor protein expression in
human endothelial cells (ratio/GAPDH)

Fig. 2. Effects of pitavastatin, sirolimus, and paclitaxel on human
CASMC proliferation and human AEC tissue factor expression.

A, PDGF-induced proliferation (% increase in cell number) of human
CASMCs. Data are the mean ± SEM ($n = 6$ each). $*p < 0.01$ versus control
by one-way ANOVA followed with Dunnett's multiple comparison test. B,
Thrombin-induced tissue factor protein expression in human AECs. Data
are the mean ± SEM ($n = 6$ each). $*p < 0.01$ versus thrombin alone by one-
way ANOVA followed with Dunnett's multiple comparison test.

Pitavastatin nearly normalized the sirolimus-induced
decrease in p-eNOS and p-Akt protein expression.

**Effects of Pitavastatin and Pitavastatin-NP on
Human CASMC Proliferation**

Both pitavastatin and pitavastatin-NP inhibited
the FBS-induced proliferation of human CASMC.
The inhibitory activities of pitavastatin-NP were
greater than those of 0.01, 0.1, and 1 μM pitavastatin
only (**Fig. 4**).

**Effects of Pitavastatin-NP-Eluting Stents and
Sirolimus-Eluting Stents on Neointima Formation
Four Weeks after Stent Implantation**

Two animals in the control bare metal stent

group died suddenly between weeks three and four;
therefore, these animals were excluded from angio-
graphic and histopathological analyses, which were
performed in 34 pigs (10 in the control bare metal
stent group, 12 in the FITC-NP-eluting stent group,
12 in the pitavastatin-NP eluting stent group, and 12
in the sirolimus-eluting stent group).

Quantitative coronary arteriography revealed
that (1) there was no significant difference in the coro-
nary diameter before and immediately after stent
implantation or in the stent-to-artery ratio among the
four groups and (2) the coronary diameter was less in
the control bare metal and the FITC-NP-eluting stent
sites than in the pitavastatin-NP-eluting stent and
sirolimus-eluting stent sites four weeks after stenting

P-eNOS
(ser1177)

P-Akt
(ser473)

eNOS

Akt

Sirolimus (10nM)
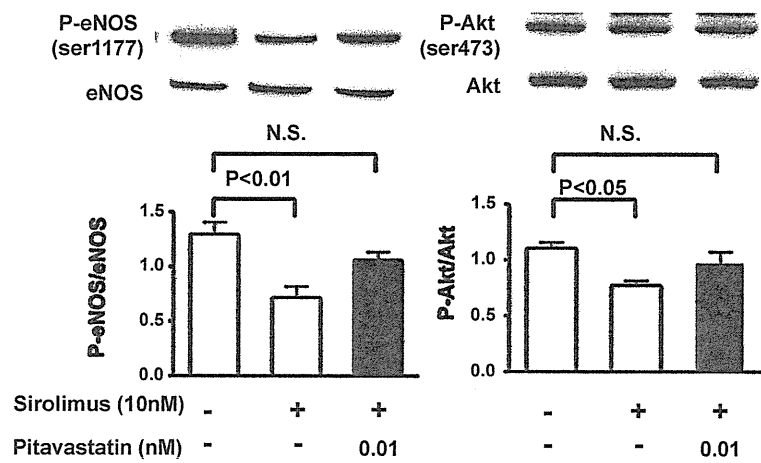
Pitavastatin (nM)

Fig. 3. Effects of pitavastatin on sirolimus-induced down regulation of eNOS and Akt (a representative down stream signal of eNOS) in human aortic endothelial cells. Pitavastatin normalized sirolimus-induced decrease in phosphorylated (activated) eNOS and Akt. Data are the mean ± SEM ($n=6$ each). $p<0.05$ or 0.01 versus no treatment by one-way ANOVA followed with Dunnett's multiple comparison test.

(Table 2). Thus, the angiographically examined in-stent stenosis was less in the pitavastatin-NP group than in the control and FITC-NP groups. The sirolimus-eluting stent showed similar inhibitory effects on markers of in-stent stenosis.

Histological analysis demonstrated that a significant in-stent neointima formed similarly at the bare metal stent and FITC-NP-eluting stent sites (Fig. 5). Quantitative analysis demonstrated that pitavastatin-NP-eluting stents attenuated in-stent neointima formation as effectively as sirolimus-eluting stents.

Effects of Pitavastatin-NP-Eluting Stents Versus Sirolimus-Eluting Stents on Inflammation and Fibrin Deposition

Micrographs of coronary artery cross-sections stained with hematoxylin-eosin from FITC-NP-eluting, pitavastatin-NP-eluting, and sirolimus-eluting stent groups are shown in Fig. 6. A semi-quantitative histological scoring system demonstrated that there was no significant difference in the injury score among the four groups four weeks after stenting (Table 3).

Inflammatory cells consisting mainly of macrophages were recruited around the stent wire and into the neointimal layer in all four sites; however, the inflammation score was significantly less at the pitavastatin-NP-eluting stent site than in the bare metal stent site (Table 3). At the sirolimus-eluting stent site, the inflammation score was greater than at the bare metal stent and pitavastatin-NP-eluting stent

FBS-induced proliferation of human coronary artery SMCs (cell number/well)
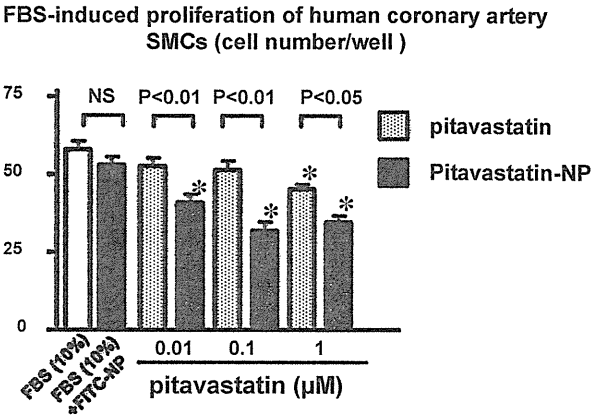
Fig. 4. Effects of pitavastatin and pitavastatin-NP on the FBS-induced proliferation of human CASMCs. Data are the mean ± SEM ($n=6$ each). $*p<0.01$ versus no treatment by one-way ANOVA followed with Dunnett's multiple comparison test.

sites (Table 3).

Minor fibrin deposition was observed at bare metal, FITC-NP-eluting, and pitavastatin-NP-eluting stent sites (Table 3). At the sirolimus-eluting stent site, the fibrin score was significantly higher than at the bare metal stent site, and this difference was even more significant when compared with the pitavastatin-NP-eluting stent site.

To determine whether the therapeutic effects of

Table 2. Coronary angiographic parameters (coronary artery diameter, in-stent stenosis) before, immediately after, and 4 weeks after stent implantation in porcine coronary artery

	BMS (n = 10)	FITC-NP stent (n = 12)	Pitavastatin -NP stent (n = 12)	SES (n = 12)	p value
Coronary diameter before stent implantation	2.19 ± 0.04	2.25 ± 0.05	2.41 ± 0.06	2.42 ± 0.10	NS
Coronary diameter immediately after stent implantation	2.70 ± 0.06	2.75 ± 0.05	2.79 ± 0.03	2.89 ± 0.04	NS
Stent-to-artery ratio immediately after stent implantation	1.20 ± 0.02	1.22 ± 0.03	1.13 ± 0.02	1.19 ± 0.04	NS
Coronary diameter 4 weeks after stent implantation	1.45 ± 0.13	1.51 ± 0.10	2.02 ± 0.12*	2.02 ± 0.15*	0.0025
Angiographically-examined in-stent restenosis 4 weeks after stent implantation (% diameter stenosis)	42.9 ± 4.9	46.0 ± 3.4	25.8 ± 3.5*	27.2 ± 3.7*	0.0003

Data are the mean ± SEM. NS = not significant
*$p < 0.05$ versus control bare metal stent by Bonferroni's multiple comparison tests

the pitavastatin-NP-eluting stent are mediated by local or systemic mechanisms, effects of intracoronary administration of pitavastatin-NP on histopathological features after deployment of bare metal stents were examined (**Table 4**). Pitavastatin-NP at 300 μg showed no therapeutic effects on indices of in-stent stenosis and adverse effects on histopathological scoring. Pitavastatin-NP at 3000 μg also had no effects on indices of in-stent stenosis, but modestly but significantly decreased fibrin deposition.

Effects of Pitavastatin-NP-Eluting Stents Versus Sirolimus-Eluting Stents on Endothelial Surface Coverage

As previously reported, re-endothelialization was not impaired at sirolimus-eluting stent sites four weeks post-stenting. There was no significant difference in the re-endothelialization score among the four groups four weeks after stenting (**Table 3**); therefore, the endothelial surface coverage was examined at earlier time points (seven days post-stenting) by scanning electron microscopy. At bare metal stent sites, almost complete endothelial coverage was noted above and between stent struts at seven days (**Fig. 7**). Similar magnitudes of endothelial coverage were observed at FITC-NP-eluting stent and pitavastatin-NP-eluting stent sites. In contrast, endothelial coverage was impaired at sirolimus-eluting stent sites; regions lacking endothelial coverage were generally associated with platelet aggregation and adherent leukocytes.

Serum and Tissue Concentrations of Pitavastatin

Tissue concentrations of pitavastatin were below the limit of detection (2.5 ng/g protein) in coronary artery segments three hours after the deployment of pitavastatin-NP-eluting stents. In addition, serum levels of pitavastatin were below the limit of detection (1 ng/mL) one and three hours after the deployment of pitavastatin-NP-eluting stents.

Discussion

We here report the first successful development of pitavastatin-NP-eluting stents with a newly invented cationic electrodeposition coating technology. We previously showed that (1) PLGA-NP was taken up actively by VSMC and endothelial cells mainly via endocytosis and was retained stably in the intracellular space and that (2) NPs may slowly release encapsulated drugs as PLGA is hydrolyzed[22, 23] This bioabsorbable polymeric NP-eluting stent system has unique aspects with respect to vascular compatibility and efficient drug delivery (stable delivery of NPs into the neointima and medial layers until day 28 after deployment of the NP-eluting stent), as compared to dip-coated polymer-eluting stents[22]. Importantly, this NP drug delivery system can carry hydrophilic agents such as statins, which offer advantages over the current stent-coating technology. In addition, this NP-eluting stent system provided an effective means of delivering NP-incorporated drugs or genes that target intracellular proteins involved in the pathogenesis of